


## RESEARCH ARTICLE

# Preoperative function-specific connectome analysis predicts surgery-related aphasia after glioma resection

Sebastian Ille<sup>1,2</sup>  | Haosu Zhang<sup>1</sup> | Lisa Sogerer<sup>1</sup> | Maximilian Schwendner<sup>1</sup> | Axel Schöder<sup>1</sup> | Bernhard Meyer<sup>1</sup> | Benedikt Wiestler<sup>3</sup> | Sandro M. Krieg<sup>1,2</sup> 

<sup>1</sup>Department of Neurosurgery, Klinikum rechts der Isar, School of Medicine, Technical University of Munich, Munich, Germany

<sup>2</sup>TUM-Neuroimaging Center, Technical University of Munich, Munich, Germany

<sup>3</sup>Department of Diagnostic and Interventional Neuroradiology, Klinikum rechts der Isar, School of Medicine, Technical University of Munich, Munich, Germany

## Correspondence

Sandro M. Krieg, Department of Neurosurgery, Klinikum rechts der Isar Technische Universität München, Ismaninger Street 22, 81675 Munich, Germany.

Email: [sandro.krieg@tum.de](mailto:sandro.krieg@tum.de)

## Abstract

Glioma resection within language-eloquent regions poses a high risk of surgery-related aphasia (SRA). Preoperative functional mapping by navigated transcranial magnetic stimulation (nTMS) combined with diffusion tensor imaging (DTI) is increasingly used to localize cortical and subcortical language-eloquent areas. This study enrolled 60 nonaphasic patients with left hemispheric perisylvian gliomas to investigate the prediction of SRA based on function-specific connectome network properties under different fractional anisotropy (FA) thresholds. Moreover, we applied a machine learning model for training and cross-validation to predict SRA based on preoperative connectome parameters. Preoperative connectome analysis helps predict SRA development with an accuracy of 73.3% and sensitivity of 78.3%. The current study provides a new perspective of combining nTMS and function-specific connectome analysis applied in a machine learning model to investigate language in neurooncological patients and promises to advance our understanding of the intricate networks.

## KEYWORDS

connectome, DTI, graphic analysis, nTMS, surgery-related aphasia

**Abbreviations:** A, average degree; AAT, Aachener aphasia test; CPS, cortical parcellation system; DCS, direct cortical stimulation; DTI, diffusion tensor imaging; EG, global efficiency; EHI, Edinburgh Handedness Inventory; EL, local efficiency; FA, fractional anisotropy; FAT, fractional anisotropy threshold; FLT, fiber length threshold; FT, fiber tracking; NA, no aphasia; NEG, negative nTMS stimulation regions; nTMS, navigated transcranial magnetic stimulation; POS, positive nTMS stimulation regions; SRA, surgery-related aphasia; VR, visualized ratio.

Sebastian Ille and Haosu Zhang contributed equally to this study.

## 1 | INTRODUCTION

Previous studies on brain structures involved in language networks have demonstrated the inter-individual variations of cortical and subcortical language regions (Dehaene et al., 1997; Shaywitz et al., 1995; Tzourio-Mazoyer et al., 2004; Voets et al., 2019). Recent findings on language refer more to the individual level analysis (Ardila et al., 2016),

This is an open access article under the terms of the [Creative Commons Attribution-NonCommercial-NoDerivs](https://creativecommons.org/licenses/by-nc-nd/4.0/) License, which permits use and distribution in any medium, provided the original work is properly cited, the use is non-commercial and no modifications or adaptations are made.

© 2022 The Authors. *Human Brain Mapping* published by Wiley Periodicals LLC.

contributing to the modern concept of individualized treatment and function-specific glioma resection, aiming to maximize glioma resection, an important prognostic marker for these patients. However, for patients with left-sided perisylvian glioma, surgery-related aphasia (SRA) is still a common risk of surgery (Negwer et al., 2018; Sollmann et al., 2019). When the glioma is localized in eloquent regions, different functional outcomes were observed defined by critical areas preserved during surgery (Sollmann et al., 2020). With this in mind, identification of biomarkers that can predict the risk of SRA before surgery is pivotal to improve treatment plans and to preserve language function, while still aiming for a gross total resection.

The application of preoperative navigated transcranial magnetic stimulation (nTMS)-based diffusion tensor imaging (DTI) tractography combined with intraoperative direct cortical stimulation (DCS) language mapping was increasingly adopted to investigate the correlation of the network and language deficits with the aim of reducing risks of SRA (Ille et al., 2016; Ille, Sollmann, Hauck, Maurer, Tanigawa, Obermueller, Negwer, Droese, Boeckh-Behrens, et al., 2015a; Ille, Sollmann, Hauck, Maurer, Tanigawa, Obermueller, Negwer, Droese, Zimmer, et al., 2015b; Picht et al., 2013; Tarapore et al., 2012). Previous studies on this topic focused on detecting the nodes and tracts related to SRA. For instance, a cut-off distance between lesions and the arcuate fascicle (AF) set at 16 mm was associated with SRA (Sollmann et al., 2020). Likewise, the inferior fronto-occipital fascicle (IFOF), the frontal aslant tract (FAT), and the superior longitudinal fascicle (SLF)/AF were correlated with the corresponding status of language function preoperatively, postoperatively, and at follow-up (Ille et al., 2018).

The current view considers cerebral language function being produced and underpinned by dynamic interactions within and between specialized brain networks (Shafto & Tyler, 2014). It demonstrated that it is not enough to understand cerebral function from the composition of language-related brain structures alone. It should also consider aspects of the network performance as well. Mbwana's findings in 2009 demonstrated that the individual language-related network was different at certain levels of network reorganization in localization-related epilepsy (Mbwana et al., 2009). In 2019, language network's different individual performances were detected by Voets and colleagues, showing the functional connectivity of brain regions involved in language fluency. This study identified "fingerprints" of brain plasticity in individual patients (Voets et al., 2019). Their experimental method was based on functional MRI (fMRI) to investigate the changes in the language network. In contrast, studies by Chang et al. were based on DTI tractography, which developed the understanding of the anatomical and functional language network (Chang et al., 2015). Notably, this study focused on the relationship between the network and functional performances. However, it did not investigate the characteristics of the network itself, including network efficiency and average degrees.

nTMS language mapping defines positive and negative sites according to whether the stimulation induces language errors. Previous studies mostly focused on positive sites and related tracts to investigate their corresponding functional alteration. However, there has been little agreement on understanding the networks' properties corresponding to positive and negative mapping regions to date. We

investigated not only the intra-network properties of the mapped sites, but also the network of brain regions connected to those sites. It provides a comprehensive perspective of the function of these mapped sites in the network and facilitates our understanding on the role of intra- and cross-hemispheric connectivity and their corresponding networks in language performance.

The objectives of this present study are to determine preoperative risk factors for early postoperative SRA in patients with language-eloquent glioma based on (1) the changes of structural network characteristics, (2) the differences between nTMS language-positive and language-negative sites in patients with and without SRA, (3) differences between the network characteristics of nTMS language-positive and language-negative sites, and (4) the comparisons of the network of brain regions connecting mapping sites with the internal network of mapping sites.

## 2 | MATERIALS AND METHODS

### 2.1 | Ethical approval

The current study followed the Declaration of Helsinki and its later amendments and was approved and supervised by the local ethic committee of the Technical University Munich (registration number 222/14 and 192/18). All patients gave written informed consent to participate in this study.

### 2.2 | Inclusion criteria and demographic data collection

The present study is a post hoc analysis of 60 patients with unaffected preoperative language function. Thirty patients developed SRA lasting more than 1 month after the operation (Group SRA) and 30 patients did not show postoperative aphasia (Group NA).

The following inclusion criteria were defined for the current study:

1. Age above 18 years.
2. German as first language.
3. Left-sided gliomas inside or adjacent to left-sided perisylvian regions or the arcuate fasciculus
4. Preoperative MRI-imaging: T1-weighted image and a DTI scan with 32 diffusion directions.
5. Preoperative nTMS language mapping.
6. Clinical language follow-up performed more than 1 month after the operation.

The exclusion standards were as follows:

1. Neurological or psychiatric diseases (except for the diagnosis of glioma).
2. Preoperative aphasia.
3. Biopsy only.

## 2.3 | MRI and clinical testing

Preoperative MRI scans (Achieva 3T, Philips Medical System) were acquired during routine imaging, including DTI (TR/TE: 5000/78 ms, voxel size of  $2 \times 2 \times 2 \text{ mm}^3$ , 32 diffusion gradient directions,  $b$ -value  $1000 \text{ s/mm}^2$ ) and T1-weighted with contrast agent (TR/TE: 9/4 ms,  $1 \text{ mm}^3$  iso-voxel; Dotagraf 0.5 mmol/ml, produced by Jenapharm GmbH & Co. KG).

According to the Aachener aphasia test (AAT), the aphasia level was rated before the operation and 1 month postoperatively (Biniek et al., 1992). For the present analysis, data were reviewed by a speech therapist, leading to the categorization of aphasia levels according to the classification in the AAT (0 = no impairment of language function; 1 = slight impairment of daily communication; 2 = moderate impairment of language function, daily communication possible; 3 = severe impairment of language function, daily communication not possible; A = nonfluent; B = fluent). Afterwards we binarized the patients' language status to SRA and NA depending on the comparison of evaluations pre- and postoperatively. The handedness of patients was analyzed using the Edinburgh Handedness Inventory (EHI; Oldfield, 1971).

## 2.4 | nTMS language mapping

Preoperative nTMS language mapping was performed following processes established in previous studies and according to our standard protocol (Ille, Sollmann, Hauck, Maurer, Tanigawa, Obermueller, Negwer, Droese, Boeckh-Behrens, et al., 2015a; Ille, Sollmann, Hauck, Maurer, Tanigawa, Obermueller, Negwer, Droese, Zimmer, et al., 2015b; Picht et al., 2013). T1 images were imported to the Nexstim eXimia NBS system (version 5.1.1; Nexstim Plc) for navigating the targeted stimuli (Ille & Krieg, 2021; Picht et al., 2013). According to the cortical parcellation system (CPS), stimulation with 100% resting motor threshold intensity was targeted at 46 regions predefined on the left hemisphere. Comparing the patients' object naming task performance in the session under stimulation (stimulation session) to the session without nTMS stimulation (baseline session), the regions corresponding to language errors were identified as language-positive regions (POS) and language-negative regions (NEG). Both were then exported as DICOM files. With respect to the intraoperative use of nTMS data, the mapping of the tumor hemisphere had priority.

## 2.5 | Connectome construction

Image files were transformed to NIFTI format (dcm2niix. <https://github.com/rordenlab/dcm2niix>). For individualized analysis, B0 was extracted from the DTI file for registration. First, each gradient direction from the DTI was linearly registered onto the B0 image (Figure 1). Second, the T1w image was skull-stripped (HD-bet, <https://github.com/MIC-DKFZ/HD-BET/>), then linearly registered to the B0 image (Isensee et al., 2019), during which transformation datasets of the

conversion process were generated. Because the POS and NEG were constructed based on the space as T1w, POS and NEG were registered to the B0 image applying the same transformation datasets. In the end, the atlas template AAL90 was deformably also registered to the B0 image. This registration enabled the cerebral structures to be individually identified, through which atlas regions corresponding to mapping points can be identified in POS and NEG images, respectively.

Next, whole brain tractography was constructed (Python library DIPY, Version 1.2.0, <https://dipy.org>). The constrained spherical deconvolution (CSD) model was applied (Figure 1I). Then a deterministic algorithm was used for fiber tracking (FT) under a series of the fractional anisotropy thresholds (FAT) that were started from 0.0 and increased by 0.01 with a fiber length threshold (FLT) set at 30 mm (Song et al., 2014) to exclude U-fibers. Individual FT stopped when a minimum count of fibers was visualized, and the corresponding FAT was at the maximum value ( $FAT_{max}$ ). During this process, the maximum FA for every single fiber was recorded as  $fa_{max}$ , and its FA ratio (VR) was calculated by the formula:

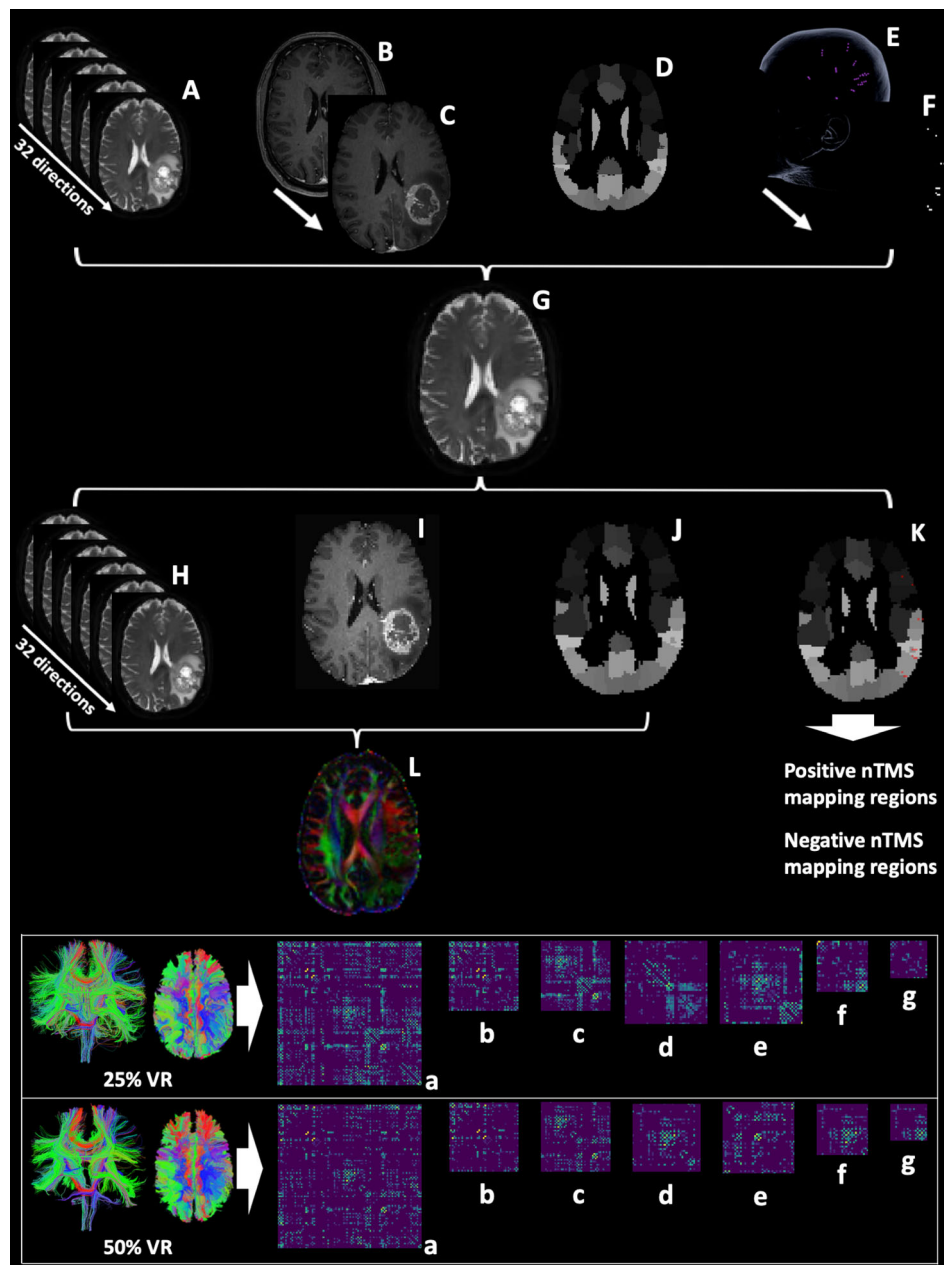
$$VR = \frac{fa_{max}}{FA_{max}} \times 100\%$$

Connecting fibers with  $VR \geq 25\%$  and  $\geq 50\%$  (Figure 1) were selected according to the corresponding nodes used in the following seven connectomes:

1.  $M_{whole}$ : the matrix (M) with nodes from both hemispherical regions according to the template AAL90 at the size of 90 nodes  $\times$  90 nodes.
2.  $M_{left}$ : M with nodes from the left hemispherical regions according to the template AAL90 at the size of 45 nodes  $\times$  45 nodes.
3.  $M_{right}$ : M with nodes from the right hemispherical regions according to the template AAL90 at the size of 45 nodes  $\times$  45 nodes.
4.  $M_{pos-rela}$ : M with nodes from the positive language mapping regions and the regions connected to them according to the template AAL90.
5.  $M_{neg-rela}$ : M with nodes from the negative language mapping regions and the regions connected to them according to the template AAL90.
6.  $M_{pos}$ : M with nodes from the positive language mapping regions according to the template AAL90.
7.  $M_{neg}$ : M with nodes from the negative language mapping regions according to the template AAL90.

Because the individual brain and tumor sizes were variable, binarization was applied to minimize their impacts. Likewise, connections between two respective regions in the connectome were transformed depending on whether the fiber counts were  $\geq 3$  or not.

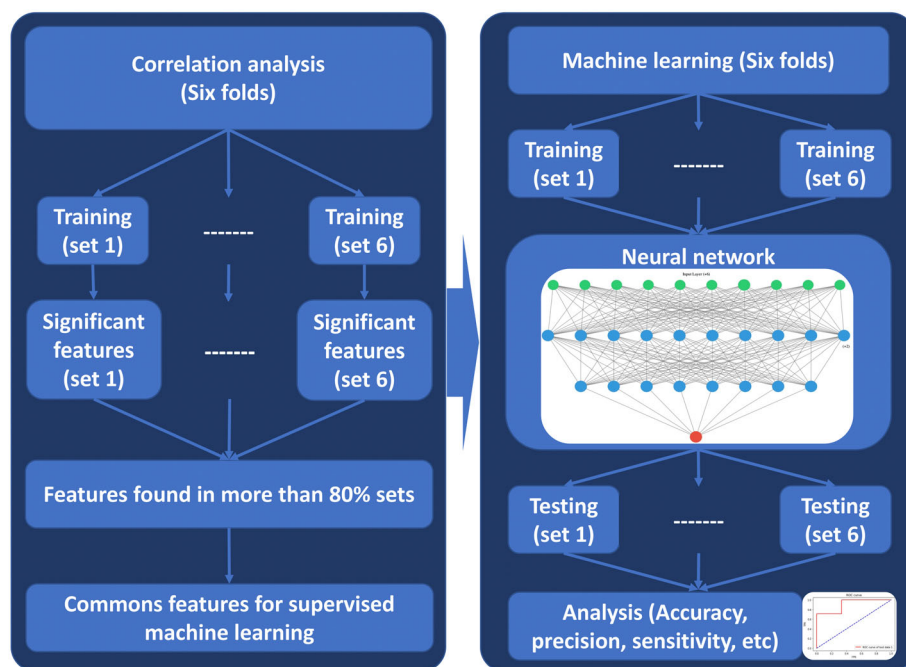
The metrics representing the graphic properties of the connectomes were analyzed through the NetworkX 2.5 library (<https://networkx.org/>) in Python 3.7 (<https://www.python.org/>), consisting of (1) the average degree (AD): the number of edges compared to the



**FIGURE 1** This figure shows the workflow of MRI processing in network construction. Figure A represents DTI scans with 32 directions. Figure C is the skull-stripped MRI (T1 with contrast) derived from Figure B through HD-bet. Figure D is the AAL90 template, and figures E and F show nTMS data. Figure A, C, D, and F are registered to the B0 (Figure G). Figure H contains the registered DTI, Figure I contains registered T1 with contrast, Figure J shows the registered AAL90 template, and Figure K shows the registered nTMS data (positive and negative regions). Then, tractography based on the CSD model applying deterministic fiber tracking thresholding at a visualization ratio (VR) of 25% and 50% was performed to generate respective connectomes. In the next step, connectomes for further analysis were constructed based on different nodes and connections as the following: (1)  $M_{whole}$  (a): the matrix (M) with nodes from both hemispherical regions according to the template AAL90 at the size of 90 nodes \* 90 nodes. (2)  $M_{left}$  (b): M with nodes from the left hemispherical regions according to the template AAL90 at the size of 45 nodes \* 45 nodes. (3)  $M_{right}$  (c): M with nodes from the right hemispherical regions according to the template AAL90 at the size of 45 nodes \* 45 nodes. (4)  $M_{pos-rela}$  (d): M with nodes from the positive language mapping regions and the regions connected to them according to the template AAL90. (5)  $M_{neg-rela}$  (e): M with nodes from the negative language mapping regions and the regions connected to them according to the template AAL90. (6)  $M_{pos}$  (f): M with nodes from the positive language mapping regions according to the template AAL90.  $M_{neg}$  (g): M with nodes from the negative language mapping regions according to the template AAL90

number of nodes representing the connecting density (Latora & Marchiori, 2001; Wang et al., 2010); (2) the average shortest path lengths (AL): the average of the smallest number of edges in the path between two nodes in the whole network, indicating its intensity and

density of connections (Rutter et al., 2013; Zhang et al., 2021); (3) global efficiency (EG): to measure the efficiency of parallel information transfer and integrated processing (Latora & Marchiori, 2001; Wang et al., 2010); and (4) local efficiency (EL): to estimate the



**FIGURE 2** This figure presents the workflow of the sixfold cross-validation machine learning for predicting the postoperative language functions. First, common features are defined as to be significantly correlated to the postoperative language levels in more than 80% of the six training sets. Second, those parameters were used for the cross-validation machine learning using neural network, in which the model was generated, and its performance was assessed, including accuracy, precision.

efficiency of communication between neighbors of a node when that node is eliminated (Latora & Marchiori, 2001; Wang et al., 2010). Connectomics figures were created in Matlab (R2016b, Academic License to TUM) using BrainNetViewer (Xia et al., 2013).

## 2.6 | Statistical analysis

The following statistical analyses were performed with GraphPad Prism (Version 8.4.3): (1) Baseline characteristics: the comparisons of the NA and SRA groups using the Chi-square test for handedness, gender, and histopathological diagnosis. Independent t-testing was applied for the comparison of age and glioma size. (2) Intra- and inter-group mapping region analysis was performed by Chi-Square or Fisher Exact testing. (3) Calculation of the intra-group ratio of language mapping regions. (4) Inter-group comparisons of the network properties from different connectomes. (5) Connectome parameters were used to train a six-fold cross-validated multi-layer perceptron (with  $12 > 6 > 1$  units and sigmoid output) to predict SRA (Figure 2).

## 3 | RESULTS

### 3.1 | Demographic analysis

There were no differences of age between the NA group ( $59.7 \pm 15.1$  years) and SRA group ( $58.8 \pm 15.2$  years;  $p = .327$ ). The comparison of tumor size in NA group ( $2.438 \pm 2.630$  cm<sup>3</sup>) and SRA group ( $2.829 \pm 2.853$  cm<sup>3</sup>) showed no difference ( $p = .583$ ; Table 1). The Chi-square test showed no difference for handedness, gender, and WHO grade between the NA and SRA group (Table 1). The  $FAT_{max}$

values of both groups were comparable with  $0.531 \pm 0.065$  for the NA and  $0.545 \pm 0.053$  for the SRA group ( $p = .378$ ; Table 1).

### 3.2 | Mapping region analysis

The number of POS regions was significantly lower than NEG regions in both groups ( $p < .001$ , Figure 3), without differences between the NA and SRA groups regarding the number of POS and NEG regions. There were no differences of objects numbers detected after regarding baseline tests ( $p = .921$ ).

The intragroup analysis of overlapping regions detected in more than 20 patients per group (>66.7%) is presented in Table 2. The frontal superior gyrus was positively mapped in 20 patients from the NA group but only in 15 patients of the SRA group. The triangular parts of the frontal inferior gyrus and the parietal inferior gyrus were negatively mapped in 20 and 22 patients of the SRA group but only in 16 and 18 NA patients, respectively (Table 2). There were no significant differences for the number of mapping regions between NA and SRA groups (Table S2).

### 3.3 | Average degree and shortest path length analysis

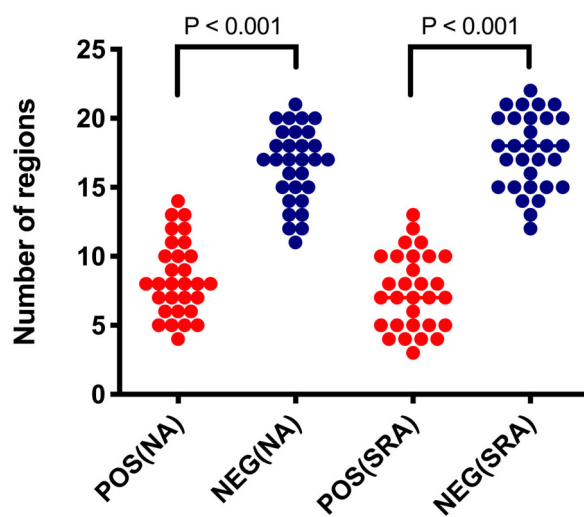
Generally, ADs were higher in the NA group than in the SRA group thresholding at 25% and 50% VR, in which the comparisons of ADs from the  $M_{right}$ ,  $M_{pos-rela}$ , and  $M_{pos}$  between the NA group and the SRA group showed statistically significant differences (25% VR:  $p = .044$ ,  $p = .040$ ,  $p = .045$ ; 50% VR:  $p = .031$ ,  $p = .018$ ,  $p = .046$ ; Table 3; Figure 4). Only at 50% VR, the  $M_{whole}$  and  $M_{left}$  showed

**TABLE 1** Patient characteristics

Items						Chi-square	p-value
Handedness	Left	NA	4	Right	NA	0.131	.718
		SRA	5		SRA		
Gender	Male	NA	6	Female	NA	2.052	.152
		SRA	11		SRA		
WHO	I-II	NA	8	III-IV	NA	0.089	.766
		SRA	7		SRA		
Age	NA: 59.7 ± 15.1 years		SRA: 58.8 ± 15.2 years		P:	.327	
					T:		.988

Note: This table presents the Chi-square testing of patient characteristics, including handedness, gender, and WHO (World Health Organization) grade of glioma. No difference was detected between the two groups without aphasia (NA) and with surgery-related aphasia (SRA).

### The number of nTMS mapping regions



**FIGURE 3** The figure shows that the number of positive mapping regions (in red) was significantly lower than the negative mapping regions (in blue) in both groups compared by paired t-testing. No differences were found for the number of mapping regions between the NA (no aphasia, show as “o”) and the SRA (surgery-related aphasia, show as “●”) group.

higher AD in the NA group ( $p = .023$ ,  $p = .037$ ; Table 3; Figure 4). Regarding the path length, AL from the  $M_{right}$  is significantly smaller in NA group ( $p = .021$ ; Table 3; Figure 4).

### 3.4 | Efficiency analysis

The connectome efficiencies EG and EL averages were higher in the NA group than those of the SRA group. Efficiencies from  $M_{neg-rela}$  showed no significant difference between the two groups. The NA group had statistically higher EG and EL based on  $M_{whole}$  under both 25% and 50% VR as compared to the SRA group (Figure 4; Table 3). The EL of  $M_{left}$  showed a difference between the two groups, while the difference in EG did only appear with 25% VR (Figure 4; Table 3).

The  $M_{pos-rela}$  and  $M_{pos}$  showed more EG under both VR thresholds in the NA group. However, their ELs were without significant differences (Figure 4; Table 3). EL from  $M_{neg}$  with 50% VR was significantly lower in the SRA group (Figure 4; Table 3).

### 3.5 | Correlation and machine learning analysis

Based on the ROC analysis, EG from  $M_{whole}$  and  $M_{left}$ , EL from  $M_{left}$ , and AL from  $M_{right}$  under 25% VR were statistically significant ( $p = .020$ ,  $p = .027$ ,  $p = .013$ , and  $p = .025$ ; Table 4). Moreover, at 50% VR, additional graphic properties were found to be statistically significant ( $M_{pos-rela}$ -EG,  $M_{pos}$ -EG,  $M_{whole}$ -EG,  $M_{right}$ -EG,  $M_{left}$ -EL,  $M_{whole}$ -EL,  $M_{whole}$ -AD,  $M_{left}$ -AD,  $M_{right}$ -AD, and  $M_{pos-rela}$ -AD; Table 4).  $M_{whole}$ -EG and  $M_{pos-rela}$ -EG showed the highest sensitivity (0.733) and specificity (0.600) compared to other graphic properties.  $M_{whole}$ -AD,  $M_{left}$ -AD,  $M_{right}$ -AD, and  $M_{pos-rela}$ -AD showed high sensitivity (>0.800) at a lower specificity between 0.433 and 0.567, leading to the high risk of false-negative differentiation.

In the cross-validation machine learning model, the average of Accuracy, Precision, Sensitivity, and area under the curve (AUC) across six cross-validation folds are all above 70% (76.7%, 75.2%, 80.3%, and 79.9%; Table S2).

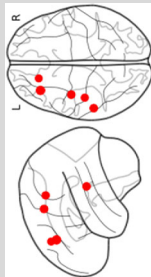
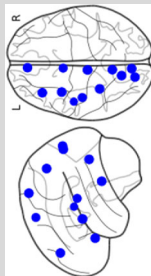

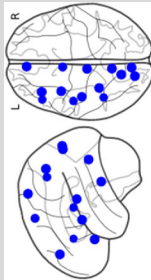
## 4 | DISCUSSION

The present study provides a new perspective to advance the investigation of language-related network properties through function-specific connectome analysis. It offers a new analysis to identify patients in the preoperative phase at risk of potentially developing postoperative SRA, using graphic analysis and a machine learning model.

### 4.1 | Prediction of SRA

Predicting SRA before surgery is a difficult point in current neurosurgery practice. Comprehensive and effective methods are needed to

TABLE 2 Analysis of mapping regions

No aphasia (NA)	Surgery-related aphasia (SRA)
<p>Ratio of overlapping positive regions</p>  <p>Ratio of overlapping negative regions</p> 	<p>Ratio of overlapping positive region</p>  <p>Ratio of overlapping negative regions</p> 
<p>Frontal middle gyrus: 93.3%</p> <p>Precuneus gyrus: 76.7%</p> <p>Temporal middle gyrus: 76.7%</p> <p>Postcentral gyrus: 70.0%</p> <p>Frontal superior gyrus: 67.7%</p>	<p>Frontal middle gyrus: 83.3%</p> <p>Temporal middle gyrus: 80.0%</p> <p>Precuneus gyrus: 73.3%</p> <p>Postcentral gyrus: 66.7%</p>
<p>Paracentral Lobule: 100%</p> <p>Fusiform gyrus: 100%</p> <p>Precuneus gyrus: 100%</p> <p>Lingual gyrus: 100%</p> <p>Cuneus gyrus: 100%</p> <p>Frontal inferior gyrus (Orb): 100%</p> <p>Insula: 100%</p> <p>Frontal superior medial gyrus: 96.7%</p> <p>Occipital superior gyrus: 96.7%</p> <p>Supplementary motor area: 86.7%</p> <p>Heschl gyrus: 86.7%</p> <p>Rolandic gyrus (Oper): 70.0%</p>	<p>Occipital superior gyrus: 100%</p> <p>Fusiform gyrus: 100%</p> <p>Precuneus gyrus: 100%</p> <p>Frontal superior medial gyrus: 100%</p> <p>Insula: 100%</p> <p>Frontal inferior gyrus (Orb): 100%</p> <p>Paracentral Lobule: 100%</p> <p>Lingual gyrus: 100%</p> <p>Cuneus gyrus: 100%</p> <p>Heschl gyrus: 96.7%</p> <p>Supplementary motor area: 83.3%</p> <p>Rolandic gyrus (Oper): 73.3%</p> <p>Parietal inferior gyrus: 73.3%</p> <p>Frontal inferior gyrus (Tri): 66.7%</p>

Note: This table shows the intragroup analysis of overlapping positive and negative mapping regions identified in more than 20 patients (>66.7%) after being registered to the AAL90 template (Mid: middle; Sup: superior; Inf: inferior; Supp: supplementary; Oper: opercular part; Tri: triangular part; Orb: orbital part). All mapping regions were located in the left hemisphere.

**TABLE 3** Analysis on average degree and efficiency analysis

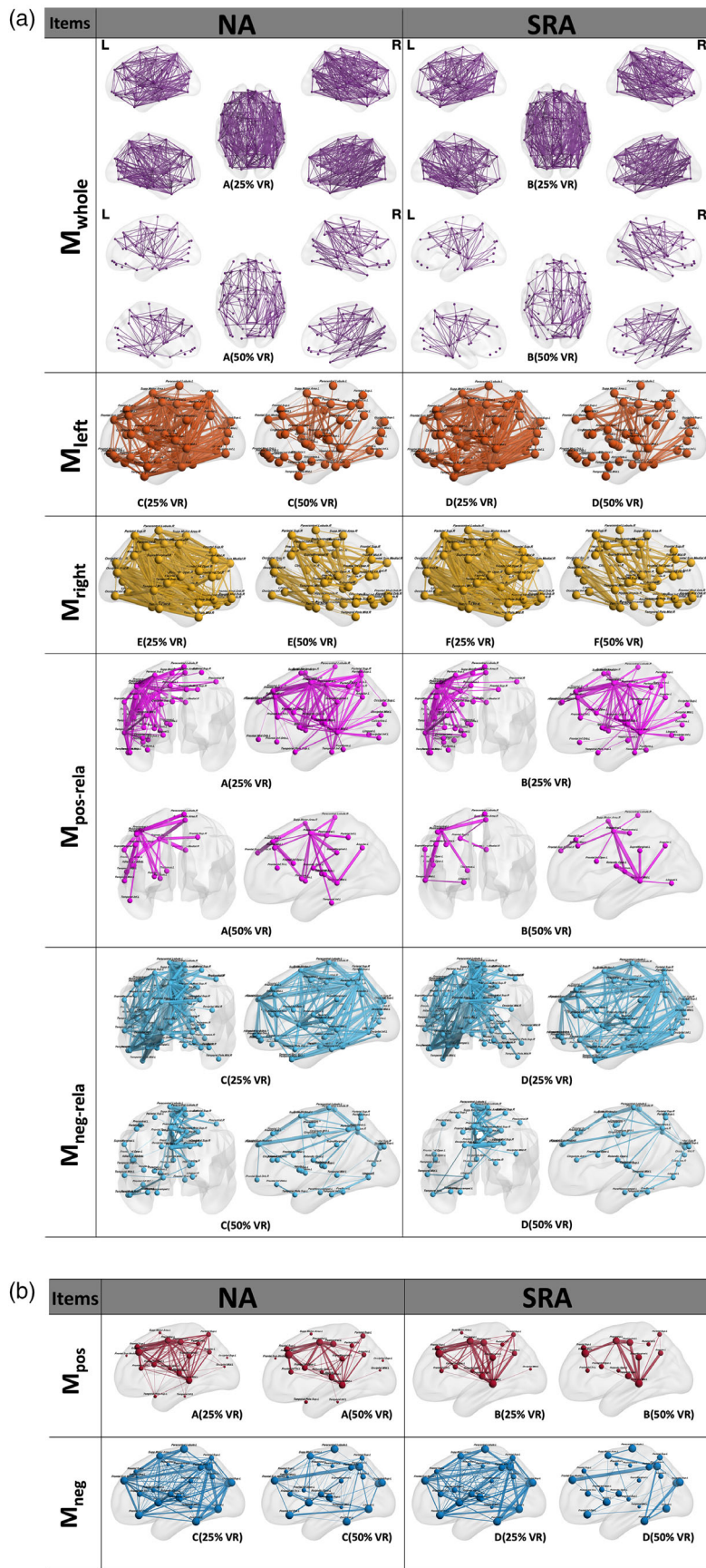
Items	Efficiency						
	M <sub>whole</sub>	M <sub>left</sub>	M <sub>right</sub>	M <sub>pos-rela</sub>	M <sub>neg-rela</sub>	M <sub>pos</sub>	M <sub>neg</sub>
25% VR							
AD							
NA	7.635	5.430	5.833	1.896	2.991	2.073	2.392
SRA	7.073	4.958	5.326	1.624	2.880	1.619	2.205
p-value	.054	.087	<b>.044</b>	<b>.040</b>	.457	<b>.045</b>	.344
AL							
NA	2.079	1.927	1.861	2.235	2.28	1.251	1.901
SRA	2.121	1.958	1.921	2.254	2.329	1.203	1.953
p-value	.091	.427	<b>.021</b>	.674	.264	.737	.587
EG							
NA	0.537	0.566	0.593	0.300	0.296	0.704	0.595
SRA	0.520	0.535	0.571	0.271	0.292	0.596	0.548
p-value	<b>.014</b>	<b>.025</b>	0.078	<b>.040</b>	.743	<b>.050</b>	.084
EL							
NA	2.863	1.883	2.344	0.733	1.105	0.682	0.633
SRA	2.358	1.466	1.914	0.552	0.960	0.556	0.586
p-value	<b>.037</b>	<b>.005</b>	.089	.122	.225	.122	.247
50% VR							
AD							
NA	2.863	1.883	2.344	0.733	1.105	0.933	0.766
SRA	2.358	1.466	1.914	0.552	0.960	0.661	0.583
p-value	<b>.023</b>	<b>.037</b>	<b>.031</b>	<b>.018</b>	.182	<b>.046</b>	.154
AL							
NA	2.804	2.424	2.547	2.437	2.807	0.942	1.474
SRA	2.934	2.437	2.411	2.288	2.884	0.617	1.48
p-value	.092	.929	.214	.319	.614	.090	.976
EG							
NA	0.330	0.297	0.371	0.105	0.121	0.437	0.227
SRA	0.289	0.246	0.314	0.079	0.105	0.323	0.160
p-value	<b>.036</b>	.064	<b>.017</b>	<b>.026</b>	.215	<b>.041</b>	.078
EL							
NA	0.367	0.332	0.373	0.133	0.127	0.338	0.174
SRA	0.306	0.261	0.307	0.098	0.087	0.187	0.086
p-value	<b>.048</b>	<b>.037</b>	.070	.095	.053	.095	<b>.026</b>

Note: This table shows differences of average degree (AD), global efficiency (EG) and local efficiency (EL) between the no aphasia (NA) group and the surgery-related aphasia (SRA) group under visual ratio (VR) thresholds of 25% and 50%. AD of matrices of regions located in the right hemisphere (M<sub>right</sub>), matrices of regions connected to nTMS positive regions (M<sub>pos-rela</sub>), and of matrices of nTMS positive regions (M<sub>pos</sub>) was higher in the NA group than in the SRA group. Under both 25% and 50% VR thresholds, EGs from matrices of whole brain regions (M<sub>whole</sub>), matrices of left hemispheric regions (M<sub>left</sub>), matrices of regions connected to nTMS positive regions (M<sub>pos-rela</sub>), matrices of nTMS negative regions (M<sub>neg</sub>), and matrices of nTMS positive regions (M<sub>pos</sub>) were higher in the NA group than in the SRA group, except from 50% VR, EGs of matrices from right hemispheric regions (M<sub>right</sub>) were higher in the NA group than in the SRA group instead of EGs from M<sub>left</sub> at a VR of 50%. ELs of M<sub>whole</sub> and M<sub>left</sub> under both 25% and 50% VR thresholds as well as ELs from M<sub>neg</sub> at a VR of 50% were higher in the NA group as well. Values written in bold highlight p-values less than .05.

assist clinical treatment decisions, in order to reduce the risk of post-operative aphasia. In the current study, network properties shown in Table 4 are significant predictors of SRA. However, using one of them

alone as a predictor cannot result in satisfactory predictive performance. When comprehensively combining them into a machine learning model, a sensitivity in predicting SRA of 78.3% (specificity of





**FIGURE 4** This figure presents the tractography of connectomes thresholding at 25% and 50% visualization ratio (VR). (a) Shows connections tracked in more than 10 patients (>33.3%) for the networks:  $M_{whole}$ ,  $M_{left}$ ,  $M_{right}$ ,  $M_{pos-rela}$ , and  $M_{neg-rela}$ . (b) Shows connections tracked in more than three patients (>10.0%) for  $M_{pos}$  and  $M_{neg}$ . Results are divided into the NA (no aphasia) and the SRA (surgery-related aphasia) group each.

**TABLE 4** ROC analysis of graphic properties

Items	AUC	Cut-off value	Sensitivity	Specificity	Youden index	p-value
25% VR						
M <sub>whole</sub> -EG	0.674	0.533	0.733	0.600	0.333	.020
M <sub>left</sub> -EG	0.667	0.572	0.70	0.600	0.300	.027
M <sub>left</sub> -EL	0.687	0.722	0.867	0.500	0.367	.013
M <sub>right</sub> -AL	0.669	1.866	0.733	0.600	0.333	.025
50% VR						
M <sub>pos-rela</sub> -EG	0.650	0.095	0.733	0.600	0.333	.046
M <sub>pos</sub> -EG	0.652	0.419	0.667	0.600	0.267	.044
M <sub>whole</sub> -EG	0.663	0.322	0.633	0.700	0.333	.030
M <sub>right</sub> -EG	0.677	0.370	0.733	0.567	0.300	.019
M <sub>left</sub> -EL	0.650	0.315	0.700	0.633	0.333	.046
M <sub>whole</sub> -EL	0.654	0.352	0.700	0.633	0.333	.040
M <sub>whole</sub> -AD	0.681	2.894	0.900	0.467	0.367	.016
M <sub>left</sub> -AD	0.647	1.822	0.800	0.567	0.367	.049
M <sub>right</sub> -AD	0.654	2.522	0.900	0.433	0.333	.040
M <sub>pos-rela</sub> -AD	0.647	0.784	0.867	0.467	0.333	.048

Note: This table presents the corresponding graphic properties' area under the curve (AUC), as well as the sensitivity and specificity with  $p < .05$  in receiver operating characteristic (ROC) curve analysis. The corresponding sensitivity and specificity of average degree (AD), global efficiency (EG) and local efficiency (EL) in predicting surgery-related aphasia (SRA) were summarized under different visual ratio (VR) thresholds for different matrices (M) including matrices of whole brain regions (M<sub>whole</sub>), matrices of left hemispheric regions (M<sub>left</sub>), matrices of right hemispheric regions (M<sub>right</sub>), matrices of regions connected to nTMS positive regions (M<sub>pos-rela</sub>), matrices of nTMS positive regions (M<sub>pos</sub>), matrices of regions connected to nTMS negative regions (M<sub>neg-rela</sub>), and matrices of nTMS negative regions (M<sub>neg</sub>).

66.7%) can be accomplished (Table S2). While encouraging, these results need to be validated in further studies.

Most of the mapped regions are similar between the two groups. Furthermore, the number and location of positive and negative mapping regions were similar between both groups. It is reasonable to see those similar cortical mapping results considering that the NA and SRA group were without clinically detectable aphasia in the preoperative testing. Hence, the impact of subcortical connections on postoperative outcome as analyzed can definitely be related to the SRA since both groups underwent tumor resection.

## 4.2 | Higher connectome efficiencies in the NA group

The lower network efficiencies were calculated from connectomes from the whole brain and left hemisphere in the SRA group at both global and local levels. The efficiencies of connectomes from M<sub>whole</sub> and M<sub>left</sub> of higher VR (>50%) and lower VR (>25%) are both affected. The impact of the left-sided glioma was not limited to one hemisphere but could also be found at the global level. In the study by Ries and colleagues, it was demonstrated that patients with brain lesions relying more on interhemispheric cooperation to select words to complete the object naming task (Ries et al., 2016), which supported that SRA patients' undermined language performance was related to reduced connections among regions. The

dual-stream theory on language function has pointed out that language processing is not a simple function of local brain regions but involves information processing and signal coordination among multiple cortical and subcortical structures (Saur et al., 2008), also emphasizing that multi-regional network collaboration is needed for executing language functions. Furthermore, a study by Schuppert and colleagues indicated that the global, fragmented neural substrates underlying local and global musical information were processed in the melodic and temporal dimensions (Schuppert et al., 2000).

Only EGs were significantly higher in M<sub>pos-rela</sub> and M<sub>pos</sub> in the NA group, again demonstrating the importance of the language-positive mapping regions and connections among them in maintaining global functional integrity. It is consistent with the results of AD analysis, which indicates that language-positive regions in terms of nTMS mapping are a part of the connectome to transfer information during the language production process. This might also explain the difference between DCS and TMS positive brain regions found in previous studies, suggesting that nTMS mostly discovers nodes and connections of language-related networks, while DCS focuses more on detecting the importance of certain regions and related fibers for language performance (Sollmann et al., 2014). The interaction of language-related cortical areas and subcortical fibers might be investigated more entirely through nTMS-based function-specific connectome analyses, which is of great significance for further research on language's structural composition.

### 4.3 | More high-VR fibers in the NA group

ADs were generally higher in the NA group than in the SRA group.  $M_{\text{pos-rela}}$  and  $M_{\text{pos}}$  under both VRs thresholds were different between the two groups but not for the  $M_{\text{neg}}$  and  $M_{\text{neg-rela}}$ .  $M_{\text{pos-rela}}$  shows the matrix consisting of positive mapping regions and their connected regions. First, from a functional point of view, it demonstrated that positive regions are essential for connecting other regions and serving as interaction centers to integrate language performance signals. Second, there are two potential reasons for higher AD in the NA group from the structural point of view. As the tumor size did not show differences between the two groups, one attribution is that patients in the SRA group rely on a weaker organization of connections initially, which ultimately leads to functional decompensation after resection. Similarly, patients in the NA group have more capability for compensation—potentially induced by glioma—to generate more connections. With this in mind, previous studies have concluded similar results indicating a higher risk of SRA in case of fewer interhemispheric connections (Negwer et al., 2018; Sollmann et al., 2017).

The tumor was localized within the left hemisphere in both groups leading to less AD as compared to the right hemisphere. The AD from fibers with VR between 25% and 50% were similar in both groups (Table S3). Significant differences in AD were shown for the connections with VR >50% (Table 3). Moreover, the investigation on the  $FAT_{\text{max}}$  shows no difference between the NA and SRA groups ( $p = .378$ ). It indicated that the fibers with higher VR (>50%) were more in the NA group than in the SRA group, which was related to the higher FA of the language-related connections. The higher FA was related to the healthy subjects' structural remodeling receiving memory learning training (Darquie et al., 2001; Sagi et al., 2012). Furthermore, it supports a study on Baduk players, who developed increased FA values in the white matter of frontal, cingulum, and striatothalamic areas after long-term training that are part of the functional networks for attentional control, working memory, executive regulation, and problem-solving (Lee et al., 2010). In the present study, the tumor's remodulation was at different levels, being lower in the SRA group than in the NA group, leading to different language prognoses.

### 4.4 | Limitation

First, no healthy subjects were enrolled as controls for the present analysis, and a bigger sample size for machine learning for predicting the postoperative language levels is still in need. Second, we have not used fMRI to identify the dominant language hemisphere, the results from left side should not be directly interpreted as dominant side effects and is only to represent the intrahemispheric effects in tumor side. Third although the Chi-square test presented no difference between the two groups in the present study, the intragroup WHO grades of glioma varied and therefore showed difference in edema size, tumor growth rate, and different extent of infiltration. Its impact on the function-specific connectome needs further studies. Fourth, further tests analyzing the neurocognitive functionality of patients

pre- and postoperatively were not conducted in the current study. We will add tests on cognitive function in the subsequent data collection for a more comprehensive analysis in order to improve the understanding of correlations to language function. Additionally, as described in the methods part of the manuscript, we finally rated aphasia levels of patients according to the final rating of aphasia in the AAT. We did not perform the entire AAT in the whole period of patient enrolment. With respect to data consistency, we used data available for all patients (according to AAT subtests "spontaneous speech" and "naming"; Table S4). Further analyses should also contain data on a more comprehensive pre- and postoperative evaluation of language function as well as a differentiation of preoperative risk factors for different levels of SRA.

## 5 | CONCLUSION

Preoperative connectome analysis can perform risk assessments predicting the development of SRA even prior to surgery. The current study provides a new perspective of function-specific connectome analysis to investigate language function in neurooncological patients. Connectome properties are a potential indicator for predicting SRA and their comprehensive combination using machine learning models predicts SRA with a sensitivity of 78.3%.

### ACKNOWLEDGMENT

Open Access funding enabled and organized by Projekt DEAL.

### FUNDING INFORMATION

This research did not receive any specific grant from funding agencies in the public, commercial, or not-for-profit sectors. This study was funded entirely by institutional grants from the department.

### CONFLICT OF INTEREST

The authors declare the existence of a financial/nonfinancial competing interest in the cover letter. All authors declare no other relationships or activities that could appear to have influenced the submitted work.

### DATA AVAILABILITY STATEMENT

Data and processing scripts involved in this study are available upon reasonable request.

### ORCID

Sebastian Ille  <https://orcid.org/0000-0003-2065-6464>

Sandro M. Krieg  <https://orcid.org/0000-0003-4050-1531>

### REFERENCES

- Ardila, A., Bernal, B., & Rosselli, M. (2016). How localized are language brain areas? A review of Brodmann areas involvement in oral language. *Archives of Clinical Neuropsychology*, 31(1), 112–122. <https://doi.org/10.1093/arclin/acv081>
- Biniek, R., Huber, W., Glindemann, R., Willmes, K., & Klumm, H. (1992). The Aachen aphasia bedside test—Criteria for validity of psychologic tests. *Nervenarzt*, 63(8), 473–479.

- Chang, E. F., Raygor, K. P., & Berger, M. S. (2015). Contemporary model of language organization: An overview for neurosurgeons. *Journal of Neurosurgery*, 122(2), 250–261. <https://doi.org/10.3171/2014.10.JNS132647>
- Darquie, A., Poline, J. B., Poupon, C., Saint-Jalmes, H., & Le Bihan, D. (2001). Transient decrease in water diffusion observed in human occipital cortex during visual stimulation. *Proceedings of the National Academy of Sciences of the United States of America*, 98(16), 9391–9395. <https://doi.org/10.1073/pnas.151125698>
- Dehaene, S., Dupoux, E., Mehler, J., Cohen, L., Paulesu, E., Perani, D., van de Moortele, P., Lehericy, S., & le Bihan, D. (1997). Anatomical variability in the cortical representation of first and second language. *Neuroreport*, 8(17), 3809–3815. <https://doi.org/10.1097/00001756-199712010-00030>
- Ille, S., Engel, L., Kelm, A., Meyer, B., & Krieg, S. M. (2018). Language-eloquent white matter pathway tractography and the course of language function in glioma patients. *Frontiers in Oncology*, 8, 572. <https://doi.org/10.3389/fonc.2018.00572>
- Ille, S., & Krieg, S. M. (2021). Functional mapping for glioma surgery, part 1: Preoperative mapping tools. *Neurosurgery Clinics of North America*, 32(1), 65–74. <https://doi.org/10.1016/j.nec.2020.08.004>
- Ille, S., Kulchyska, N., Sollmann, N., Wittig, R., Beurskens, E., Butenschoen, V. M., Ringel, F., Vajkoczy, P., Meyer, B., Picht, T., & Krieg, S. M. (2016). Hemispheric language dominance measured by repetitive navigated transcranial magnetic stimulation and postoperative course of language function in brain tumor patients. *Neuropsychologia*, 91, 50–60. <https://doi.org/10.1016/j.neuropsychologia.2016.07.025>
- Ille, S., Sollmann, N., Hauck, T., Maurer, S., Tanigawa, N., Obermueller, T., Negwer, C., Droese, D., Boeckh-Behrens, T., Meyer, B., Ringel, F., & Krieg, S. M. (2015a). Impairment of preoperative language mapping by lesion location: A functional magnetic resonance imaging, navigated transcranial magnetic stimulation, and direct cortical stimulation study. *Journal of Neurosurgery*, 123(2), 314–324. <https://doi.org/10.3171/2014.10.JNS141582>
- Ille, S., Sollmann, N., Hauck, T., Maurer, S., Tanigawa, N., Obermueller, T., Negwer, C., Droese, D., Zimmer, C., Meyer, B., Ringel, F., & Krieg, S. M. (2015b). Combined noninvasive language mapping by navigated transcranial magnetic stimulation and functional MRI and its comparison with direct cortical stimulation. *Journal of Neurosurgery*, 123(1), 212–225. <https://doi.org/10.3171/2014.9.JNS14929>
- Isensee, F., Schell, M., Pflueger, I., Brugnara, G., Bonekamp, D., Neuberger, U., Wick, A., Schlemmer, H. P., Heiland, S., Wick, W., Bendszus, M., Maier-Hein, K. H., & Kickingeder, P. (2019). Automated brain extraction of multisequence MRI using artificial neural networks. *Human Brain Mapping*, 40(17), 4952–4964. <https://doi.org/10.1002/hbm.24750>
- Latora, V., & Marchiori, M. (2001). Efficient behavior of small-world networks. *Physical Review Letters*, 87(19), 198701. <https://doi.org/10.1103/PhysRevLett.87.198701>
- Lee, B., Park, J. Y., Jung, W. H., Kim, H. S., Oh, J. S., Choi, C. H., Jang, J. H., Kang, D. H., & Kwon, J. S. (2010). White matter neuroplastic changes in long-term trained players of the game of “Baduk” (GO): A voxel-based diffusion-tensor imaging study. *NeuroImage*, 52(1), 9–19. <https://doi.org/10.1016/j.neuroimage.2010.04.014>
- Mbwana, J., Berl, M. M., Ritzl, E. K., Rosenberger, L., Mayo, J., Weinstein, S., Conry, J. A., Pearl, P. L., Shamim, S., Moore, E. N., Sato, S., Vezina, L. G., Theodore, W. H., & Gaillard, W. D. (2009). Limitations to plasticity of language network reorganization in localization related epilepsy. *Brain*, 132(Pt 2), 347–356. <https://doi.org/10.1093/brain/awn329>
- Negwer, C., Beurskens, E., Sollmann, N., Maurer, S., Ille, S., Gighuber, K., Kirschke, J. S., Ringel, F., Meyer, B., & Krieg, S. M. (2018). Loss of subcortical language pathways correlates with surgery-related aphasia in patients with brain tumor: An investigation via repetitive navigated transcranial magnetic stimulation-based diffusion tensor imaging fiber tracking. *World Neurosurgery*, 111, e806–e818. <https://doi.org/10.1016/j.wneu.2017.12.163>
- Oldfield, R. C. (1971). The assessment and analysis of handedness: The Edinburgh inventory. *Neuropsychologia*, 9(1), 97–113.
- Picht, T., Krieg, S. M., Sollmann, N., Rösler, J., Niraula, B., Neuvonen, T., Savolainen, P., Lioumis, P., Mäkelä, J. P., Deletis, V., Meyer, B., Vajkoczy, P., & Ringel, F. (2013). A comparison of language mapping by preoperative navigated transcranial magnetic stimulation and direct cortical stimulation during awake surgery. *Neurosurgery*, 72(5), 808–819. <https://doi.org/10.1227/NEU.0b013e3182889e01>
- Ries, S. K., Dronkers, N. F., & Knight, R. T. (2016). Choosing words: Left hemisphere, right hemisphere, or both? Perspective on the lateralization of word retrieval. *Annals of the New York Academy of Sciences*, 1369(1), 111–131. <https://doi.org/10.1111/nyas.12993>
- Rutter, L., Nadar, S. R., Holroyd, T., Carver, F. W., Apud, J., Weinberger, D. R., & Coppola, R. (2013). Graph theoretical analysis of resting magnetoencephalographic functional connectivity networks. *Frontiers in Computational Neuroscience*, 7, 93. <https://doi.org/10.3389/fncom.2013.00093>
- Sagi, Y., Tavor, I., Hofstetter, S., Tzur-Moryosef, S., Blumenfeld-Katzir, T., & Assaf, Y. (2012). Learning in the fast lane: New insights into neuroplasticity. *Neuron*, 73(6), 1195–1203. <https://doi.org/10.1016/j.neuron.2012.01.025>
- Saur, D., Kreher, B. W., Schnell, S., Kümmerer, D., Kellmeyer, P., Vry, M. S., Umarova, R., Musso, M., Glauche, V., Abel, S., Huber, W., Rijntjes, M., Hennig, J., & Weiller, C. (2008). Ventral and dorsal pathways for language. *Proceedings of the National Academy of Sciences of the United States of America*, 105(46), 18035–18040. <https://doi.org/10.1073/pnas.0805234105>
- Schuppert, M., Munte, T. F., Wieringa, B. M., & Altenmüller, E. (2000). Receptive amusia: Evidence for cross-hemispheric neural networks underlying music processing strategies. *Brain*, 123(Pt 3), 546–559. <https://doi.org/10.1093/brain/123.3.546>
- Shafto, M. A., & Tyler, L. K. (2014). Language in the aging brain: The network dynamics of cognitive decline and preservation. *Science*, 346(6209), 583–587. <https://doi.org/10.1126/science.1254404>
- Shaywitz, B. A., Shaywitz, S. E., Pugh, K. R., Constable, R. T., Skudlarski, P., Fulbright, R. K., Bronen, R. A., Fletcher, J. M., Shankweiler, D. P., Katz, L., & Gore, J. C. (1995). Sex differences in the functional organization of the brain for language. *Nature*, 373(6515), 607–609. <https://doi.org/10.1038/373607a0>
- Sollmann, N., Fratini, A., Zhang, H., Zimmer, C., Meyer, B., & Krieg, S. M. (2019). Associations between clinical outcome and tractography based on navigated transcranial magnetic stimulation in patients with language-eloquent brain lesions. *Journal of Neurosurgery*, 1–10, 1033–1042. <https://doi.org/10.3171/2018.12.JNS182988>
- Sollmann, N., Negwer, C., Tussis, L., Hauck, T., Ille, S., Maurer, S., Gighuber, K., Bauer, J. S., Ringel, F., Meyer, B., & Krieg, S. M. (2017). Interhemispheric connectivity revealed by diffusion tensor imaging fiber tracking derived from navigated transcranial magnetic stimulation maps as a sign of language function at risk in patients with brain tumors. *Journal of Neurosurgery*, 126(1), 222–233. <https://doi.org/10.3171/2016.1.JNS152053>
- Sollmann, N., Tanigawa, N., Ringel, F., Zimmer, C., Meyer, B., & Krieg, S. M. (2014). Language and its right-hemispheric distribution in healthy brains: An investigation by repetitive transcranial magnetic stimulation. *NeuroImage*, 102(Pt 2), 776–788. <https://doi.org/10.1016/j.neuroimage.2014.09.002>
- Sollmann, N., Zhang, H., Fratini, A., Wildschuetz, N., Ille, S., Schröder, A., Zimmer, C., Meyer, B., & Krieg, S. M. (2020). Risk assessment by pre-surgical tractography using navigated TMS maps in patients with highly motor- or language-eloquent brain tumors. *Cancers (Basel)*, 12(5), 1264. <https://doi.org/10.3390/cancers12051264>

- Song, A. W., Chang, H. C., Petty, C., Guidon, A., & Chen, N. K. (2014). Improved delineation of short cortical association fibers and gray/white matter boundary using whole-brain three-dimensional diffusion tensor imaging at submillimeter spatial resolution. *Brain Connectivity*, 4(9), 636–640. <https://doi.org/10.1089/brain.2014.0270>
- Tarapore, P. E., Tate, M. C., Findlay, A. M., Honma, S. M., Mizuiri, D., Berger, M. S., & Nagarajan, S. S. (2012). Preoperative multimodal motor mapping: A comparison of magnetoencephalography imaging, navigated transcranial magnetic stimulation, and direct cortical stimulation. *Journal of Neurosurgery*, 117(2), 354–362. <https://doi.org/10.3171/2012.5.JNS112124>
- Tzourio-Mazoyer, N., Josse, G., Crivello, F., & Mazoyer, B. (2004). Interindividual variability in the hemispheric organization for speech. *NeuroImage*, 21(1), 422–435. <https://doi.org/10.1016/j.neuroimage.2003.08.032>
- Voets, N. L., Parker Jones, O., Mars, R. B., Adcock, J. E., Stacey, R., Apostolopoulos, V., & Plaha, P. (2019). Characterising neural plasticity at the single patient level using connectivity fingerprints. *NeuroImage: Clinical*, 24, 101952. <https://doi.org/10.1016/j.nicl.2019.101952>
- Wang, J., Zuo, X., & He, Y. (2010). Graph-based network analysis of resting-state functional MRI. *Frontiers in Systems Neuroscience*, 4, 16. <https://doi.org/10.3389/fnsys.2010.00016>
- Xia, M., Wang, J., & He, Y. (2013). BrainNet viewer: A network visualization tool for human brain connectomics. *PLoS One*, 8(7), e68910. <https://doi.org/10.1371/journal.pone.0068910>
- Zhang, N., Li, K., Li, G., Nataraj, R., & Wei, N. (2021). Multiplex recurrence network analysis of inter-muscular coordination during sustained grip and pinch contractions at different force levels. *IEEE Transactions on Neural Systems and Rehabilitation Engineering*, 29, 2055–2066. <https://doi.org/10.1109/TNSRE.2021.3117286>

## SUPPORTING INFORMATION

Additional supporting information can be found online in the Supporting Information section at the end of this article.

**How to cite this article:** Ille, S., Zhang, H., Sogerer, L., Schwendner, M., Schöder, A., Meyer, B., Wiestler, B., & Krieg, S. M. (2022). Preoperative function-specific connectome analysis predicts surgery-related aphasia after glioma resection. *Human Brain Mapping*, 43(18), 5408–5420. <https://doi.org/10.1002/hbm.26014>